Available online at www.sciencedirect.com
SCIENCE DIRECT®
Chemistry and Physics of Lipids 125 (2003) 123–138
CPL CHEMISTRY AND PHYSICS OF LIPIDS
www.elsevier.com/locate/chemphyslip

Shape transformation and burst of giant POPC unilamellar liposomes modulated by non-ionic detergent $C_{12}E_8$

Blaž Babnik [a], Damjan Miklavčič [a], Maša Kandušer [a], Henry Hägerstrand [b], Veronika Kralj-Iglič [c], Aleš Iglič [a,*]

[a] *Faculty of Electrical Engineering, University of Ljubljana, Tržaška 25, SI-1000 Ljubljana, Slovenia*
[b] *Department of Cell Biology, BIOCITY, Åbo Akademi University, FIN-20520 Åbo, Turku, Finland*
[c] *Faculty of Medicine, University of Ljubljana, Lipičeva 2, SI-1000 Ljubljana, Slovenia*

Received 7 January 2003; received in revised form 16 May 2003; accepted 27 May 2003

Abstract

We studied spontaneous shape transformations and burst of 1-palmitoyl-2-oleoyl-*sn*-glycero-3-phosphatidylcholine (POPC) vesicles with exogeneously added non-ionic detergent octaethylene-glycol dodecylether $C_{12}E_8$. The addition of $C_{12}E_8$ increased the speed of the vesicle shape transformation, so that we were able to study for the first time the complete sequence of POPC vesicle shapes starting from initial spherical vesicle with long thin tubular protrusion to final shape with invagination(s). The average mean curvature of the vesicle membrane continuously decreases during this process. The shape of the invaginations is usually spherical, however also non-spherical shapes of invaginations were observed. $C_{12}E_8$ increases amplitudes of the fluctuations of the vesicle membrane. At higher concentrations in the membrane, $C_{12}E_8$ induces the membrane leakage and burst of the vesicles.

Keywords: POPC; Shape transformation; Detergent; Deviatoric energy; $C_{12}E_8$

1. Introduction

The shape transformation of giant phosphatidylcholine unilamellar liposomes has been experimentally studied in the past (Käs and Sackmann, 1991; Iglič et al., 1999; Kralj-Iglič et al., 2001b; Nomura et al., 2001; Holopainen et al., 2000, 2002; Tanaka et al., 2002). The budding transition of giant 1-palmitoyl-2-oleoyl-*sn*-glycero-3-phosphatidylcholine (POPC) bilayer vesicles to the inside leading to spherical mother vesicle and the chain of daughter endovesicles or to separate daughter endovesicles protruding to the inside can be induced via temperature variations (Käs and Sackmann, 1991). If giant 1-stearoyl-2-oleoyl-*sn*-glycero-3-phosphatidylcholine (SOPC)-sphingomyelin liposomes are treated with sphingomyelinase, the budding of small endo and exovesicles and changes in lipid lateral distribution occur (Holopainen et al., 2000). Also, the addition of La^{3+} and Gd^{3+} ions may induce different shape changes of giant unilamellar vesicles of dioleoylphosphatidylcholine (DOPC) (Tanaka et al., 2002). Recently, the transformation of POPC spherical vesicle with long thin tubular protrusion, through undulated protrusions to prolate dumbbell shape was observed for the first time (Kralj-Iglič et al., 2001b). The aim

* Corresponding author. Tel.: +386-1-4768-825; fax: +386-1-4264-630.
E-mail address: ales.iglic@fe.uni-lj.si (A. Iglič).

0009-3084/$ – see front matter © 2003 Elsevier Ireland Ltd. All rights reserved.
doi:10.1016/S0009-3084(03)00084-7

of this work was to investigate the complete shape transformation of giant POPC vesicles starting from initial vesicle with long tubular protrusion to the final shape with endovesicles. In particular, we studied the influence of non-ionic surfactant octaethylene-glycol dodecylether $C_{12}E_8$ (Prete et al., 2002; Schreier et al., 2000; Heerklotz et al., 1997; Otten et al., 2000) on the vesicle shape transformations.

2. Materials and methods

Giant phospholipid vesicles were prepared at room temperature by the modified electroformation method (Angelova et al., 1992) as described in detail elsewhere (Kralj-Iglič et al., 2001b). The vesicles were prepared from phospholipid POPC purchased from Avanti Polar Lipids, Inc. In the procedure, 20 μl of

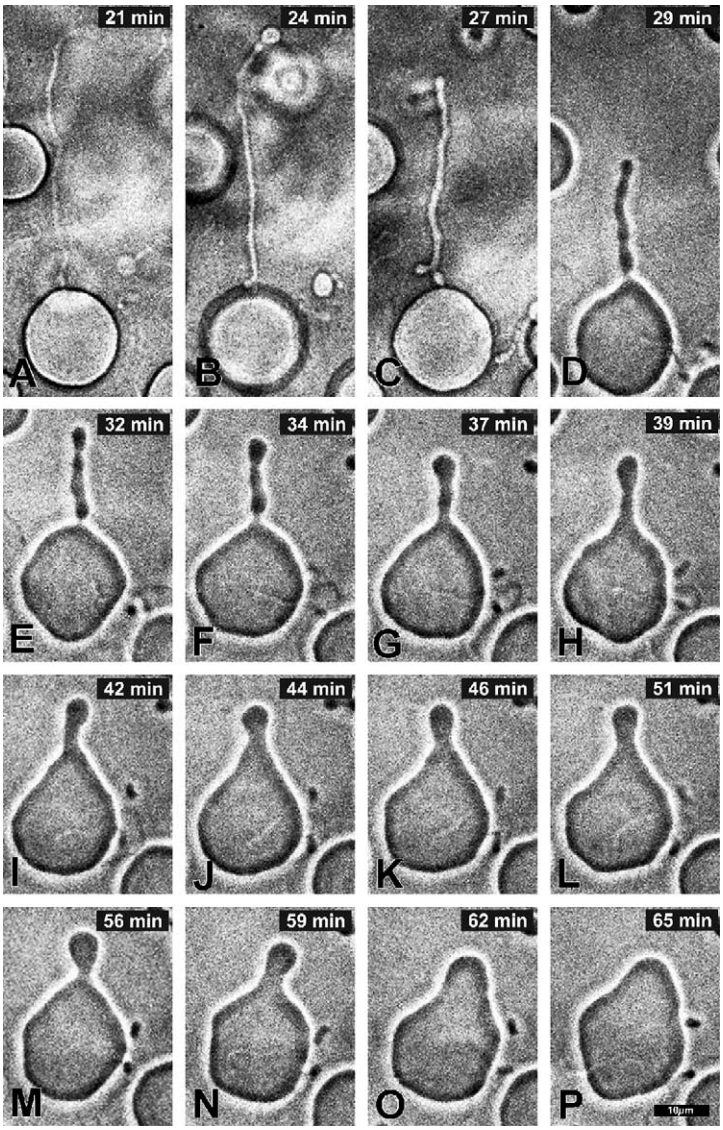

Fig. 1. Spontaneous shape transformation of the initially globular giant $C_{12}E_8$-doped POPC vesicle with long tubular protrusion. The time interval between A and P is 44 min. The bar represents 10 μm. The times after preparations of the vesicles are given in the individual micrographs.

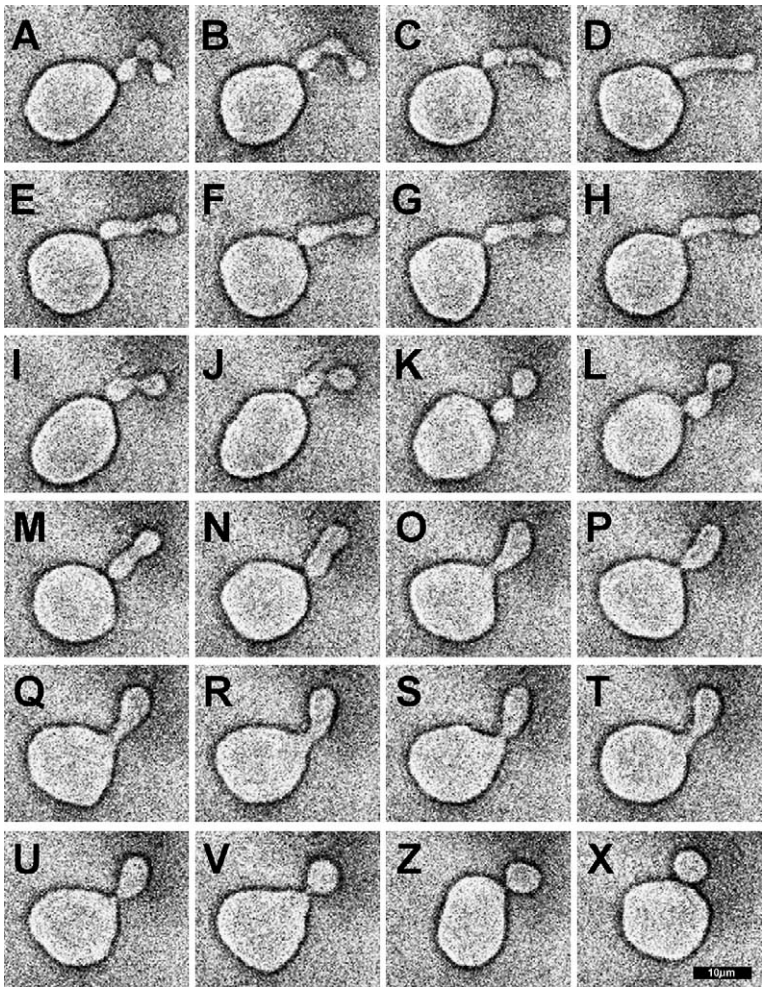

Fig. 2. Final phases of the spontaneous shortening of the initially long tubular protrusion of the giant $C_{12}E_8$-doped POPC vesicle into the outside budded vesicle (shape X). The observed vesicle composed of globular mother vesicle and three (shape A), two (shape K) and one (shape X) globular daughter vesicles (beads) connected by the very thin necks are similar to the limiting vesicle shapes (see Fig. 8b–d). The final vesicle shape (shape X) remained stable for hours. The protrusions of the shapes between the shapes A and K and the shapes between the shapes K and X have either thick connective necks between the beads composing the protrusion (shapes B, I, L) or undulated tubular character (shape G) or dumbbell character (shapes L, M). The time interval between A and X is 28 min. The bar represents 10 μm.

POPC, dissolved in 9:1 chloroform/methanol mixture, was applied to platinum electrodes. The solvent was allowed to evaporate in low vacuum for a few hours. The coated electrodes were then placed in the electroformation chamber filled with 0.2 M sucrose solution. An AC electric field with amplitude 1 V/mm and frequency 10 Hz was first applied for 2 h. Then, the amplitude and the frequency of electric field were gradually reduced (Kralj-Iglič et al., 2001b). The content of the chamber was poured out into the glass beaker and 0.2 M glucose solution was added. The suspension containing vesicles was gently mixed. In the experiment presented in Fig. 1 50 μl of the suspension containing the vesicles was placed on the cover glass, where the observation chamber was made by silicon grease. Afterwards, 10 μl of 0.186 mM $C_{12}E_8$ (Fluka, Sigma-Aldrich Chemie GmbH, CMC = 0.087 mM (Nomura et al., 2001)) aqueous solution was added directly into the observation chamber with a micropipette. The observation

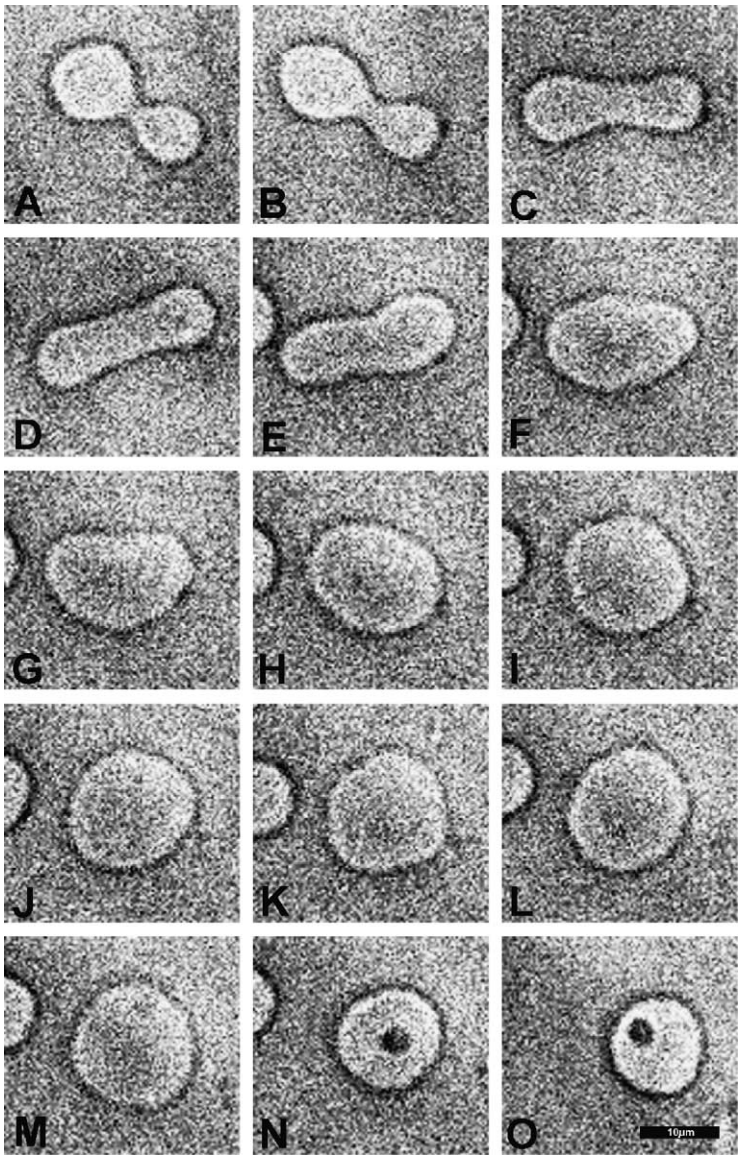

Fig. 3. Final phase of the spontaneous shape transition of the $C_{12}E_8$-doped POPC vesicle from a pear-shaped vesicle shape (shape A) to a prolate dumbbell (shape D), through non-axisymmetric (shapes F–H) and oblate vesicle shapes (shapes I–L) to the globular shape with the inner daughter vesicle (shapes N, O). The time interval between A and O is 45 min. The bar represents 10 μm.

chamber was then closed by the second cover glass. In the experiment presented in Fig. 6, the amount of 10 μl of 18.6 mM $C_{12}E_8$ solution was added into the observation chamber containing 40 μl of the suspension of vesicles. In the experiments presented in Figs. 2–5, two-compartment observation chamber was made on the cover glass using the silicon grease. The compartments were connected by very narrow channel so the contents of both compartments can be slowly mixed. In the first compartment we placed 50 μl of the suspension of vesicles while the other compartment was filled with 10 μl of 1.86 mM $C_{12}E_8$ solution. In all experiments, no coating of the glass was made. The vesicles were observed at room

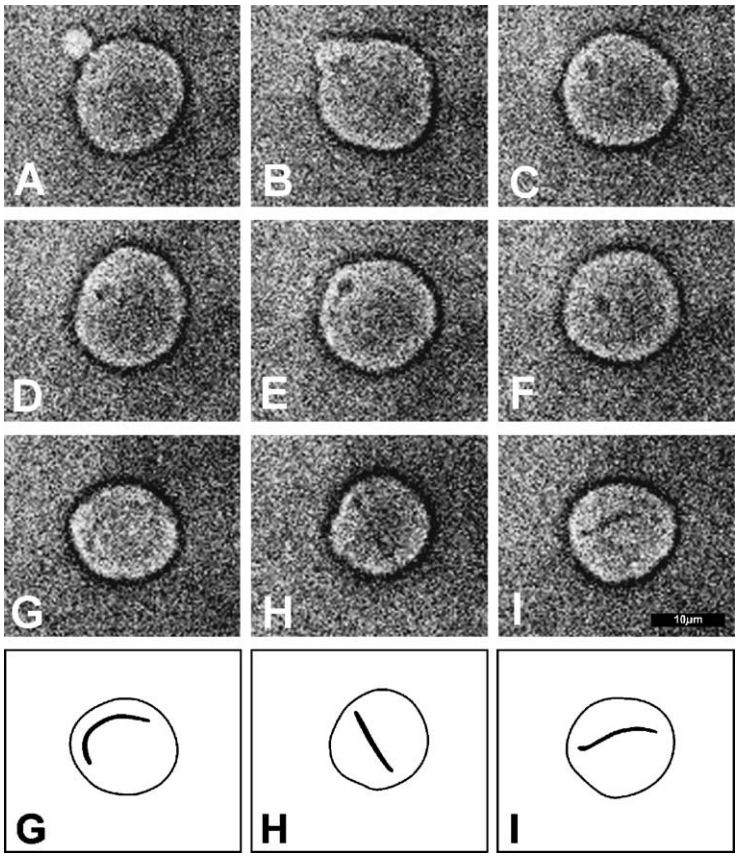

Fig. 4. Final phase of the spontaneous shape transformation of the outside budded $C_{12}E_8$-doped POPC vesicle into the inside budded vesicle with non-spherical endovesicle. The time interval between A and I is 47 s. The bar represents 10 μm.

temperature under the Zeiss 200 Axiovert inverted phase contrast microscope.

3. Experimental results

Figs. 1–4 show different phases of the shape transformations of giant $C_{12}E_8$-doped phospholipid POPC vesicles. The general features of the observed vesicle shape transformations are in some respects similar to the ones observed in pure POPC vesicles (Kralj-Iglič et al., 2001b, 2002b). Immediately after being placed into the observation chamber the vesicles are spherical and the protrusions are not visible. After some time, long thin protrusions become visible (Fig. 1A). The protrusions appear as very long thin tubes that are connected to the mother vesicle at one end while the other end is free. With time, the protrusion becomes shorter and thicker; however, the tubular character of the protrusion is still preserved (Fig. 1B and C) while the fluctuations of the mother vesicle increase in strength. Later, undulations of the protrusion appear and become increasingly apparent. Shortened protrusions look like chain of beads connected by necks (Figs. 1D–F and 2A–L). Usually the necks are thick (Figs. 1E–G and 2B, G, L). However, when the vesicle shape is close to the limiting shape composed of spherical mother vesicles and the chain of spherical daughter vesicles (see Fig. 8a–c), the globular beads forming the protrusion are connected by very thin necks (Fig. 2A, K and X). As it was already observed (Kralj-Iglič et al., 2001b) the number of beads decreases gradually one by one (Figs. 1 and 2). If the vesicle shape with the last single outside budded

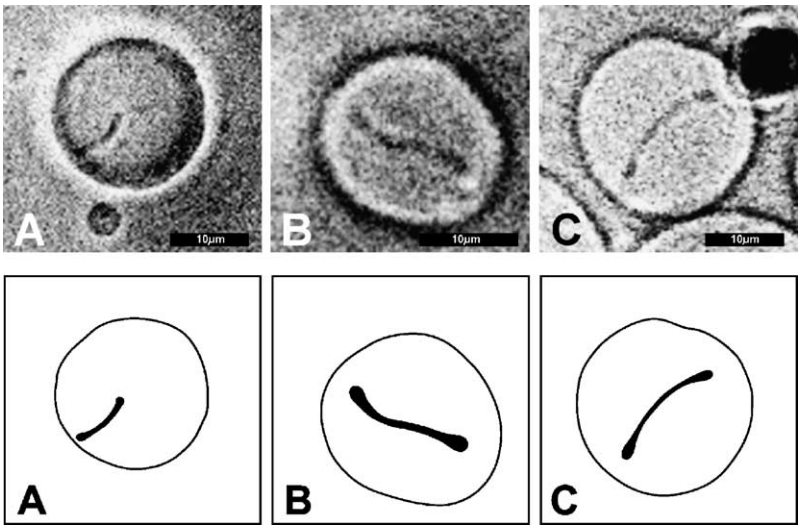

Fig. 5. Examples of the different non-spherical shapes of endovesicles formed in the final phase of the spontaneous shape transformation of the giant $C_{12}E_8$-doped POPC vesicle with initially long tubular protrusion. The bars represent 10 μm.

daughter vesicle (Figs. 1M and 2X) is not stabilized (what usually happened if the neck between the bleb and the mother vesicle is not very thin Fig. 1) the globular protrusion is completely integrated into the vesicle membrane to yield a prolate dumbbell shape (Figs. 1M–P and 3A–C). The transformation of POPC vesicles was hitherto recorded up to this point (Kralj-Iglič et al., 2001b, 2002b). The prolate dumbbell shape (Fig. 3D) may then transform into oblate shape (Fig. 3I) followed by the budding in the interior (Fig. 3N and O). The shape of invagination (inner daughter vesicle) was usually spherical (Fig. 3N and O) but could also be non-spherical, e.g. torocytic or tubular (Figs. 4G–I and 5). The same pattern of the vesicle shape transformation as presented in Figs. 1–3 has been observed in the number (more than 20) of independent experiments.

In Fig. 1, the concentration of $C_{12}E_8$ was constant and bellow CMC. In Figs. 2–4, the concentration of $C_{12}E_8$ increased with time as the concentration gradient of $C_{12}E_8$ was generated in the sample by diffusion.

At higher concentrations of $C_{12}E_8$, well above the CMC, the vesicle composed of sperical mother vesicle and spherical daughter endovesicles bursted (Fig. 6L–O) leading to the membrane solubilization (Fig. 6N and O). Before the complete solubilization, the vesicles showed membrane fluctuations and seemed to have large holes in their membrane (Fig. 6K–M). The holes are of similar shape were observed also in red blood cell ghosts (Lieber and Steck, 1982).

It was previously indicated (Kralj-Iglič et al., 2001b, 2002b; Iglič and Kralj-Iglič, 2003) that in comparing the protrusions at an early time and at a later time, the protrusions at the early time appeared considerably more tubular (see Fig. 1). Therefore, we think that the protrusions also have tubular character even at earlier times when they are too thin to be seen by the phase contrast microscope (Kralj-Iglič et al., 2001b, 2002b). The possibility should be considered that the radius of the tubular protrusion immediately after its formation is very small—as small as the membrane thickness.

It can be seen in Fig. 1 that when the protrusion is already considerably shortened (Fig. 1E–P) the mother vesicle differs from the sphere indicating that fluctuations are vigorous. The contour of the globular part exhibits straight lines separated by rather sharp edges. This behavior differs from the features in pure POPC vesicles where the mother vesicle is sphere-like with small undulations.

An interesting observed feature is oscillation of the neck width (Figs. 1 and 2) which was observed also in pure POPC vesicles (Kralj-Iglič et al., 2001b; Iglič and Kralj-Iglič, 2003; Božič et al., 2002). However, in pure POPC vesicles the neck that connects the protrusion and the mother vesicle is the thinnest and the

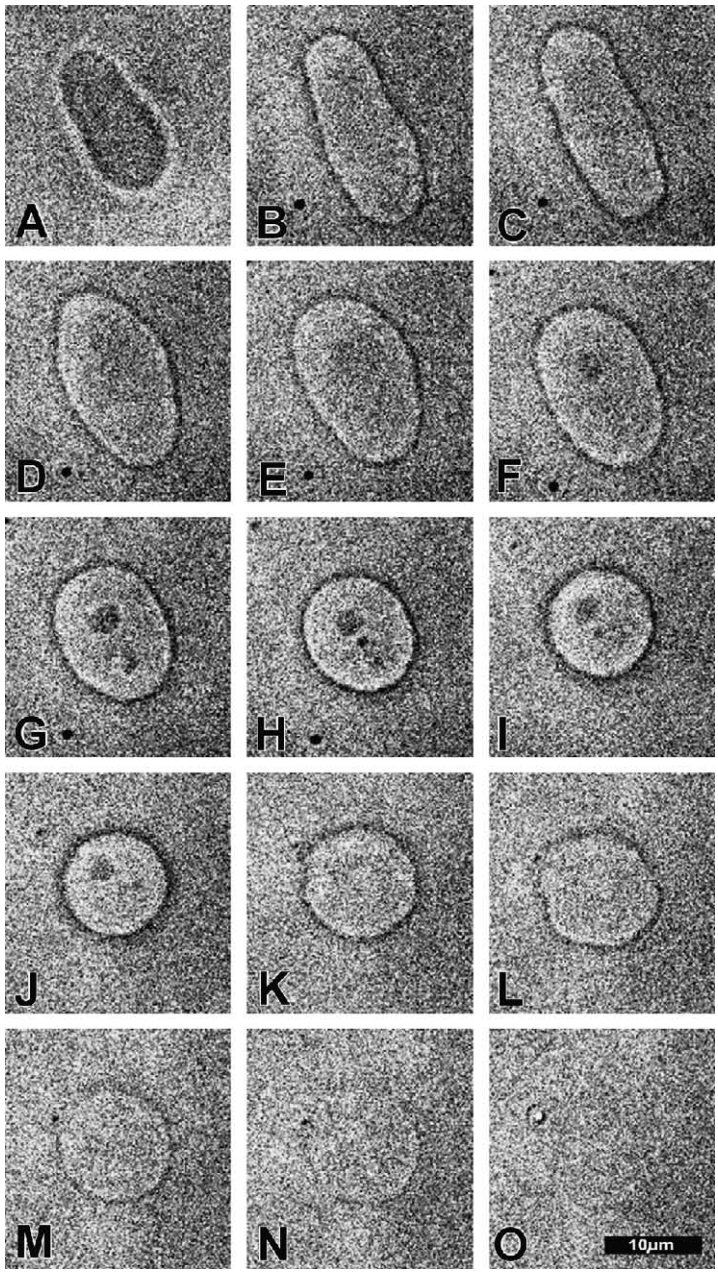

Fig. 6. Burst of globular mother vesicle with inside spherical endovesicle formed in the final phase of spontaneous shape transformation of the giant $C_{12}E_8$-doped POPC vesicle with initially long tubular protrusion. The time interval between A and O is 36 s. The bar represents 10 μm.

most stable one. In $C_{12}E_8$-doped vesicles also wider necks seem to be stable. It can be seen in Fig. 1 that thin neck that connects the protrusion and the mother vesicle opens (Fig. 1F–H) even before the wider neck connecting the two beads. The opening of the wide neck that connects the two beads follows (Fig. 1I–O). A neck shrinks and widens several times before a bead integrates with the mother vesicle

(Fig. 1L–O) indicating that the neck is energetically favorable.

A similar effect, i.e. the persistence of the neck connecting a spherical daughter vesicle and a mother vesicle, was also observed in the opening of the neck induced by cooling, while the formation of the neck by heating was quick and took place at higher temperature, indicating a hysteresis (Käs and Sackmann, 1991). If the protrusion develops spherical beads connected by very thin necks, the shape may stay stable for hours (Fig. 2X).

The shape transformation of the POPC vesicle protrusion is usually slow. In the sample, the tubular protrusions may still be observed a few hours after the formation of the vesicles. The timing of the transformation may vary from minutes to hours, as the protrusions are initially of very different lengths.

Adding the surfactant $C_{12}E_8$ in the solution increases the speed of the vesicle shape transformation. The necks of the bead-like protrusions usually seem to be thicker in the presence of $C_{12}E_8$ in comparison to the situation without $C_{12}E_8$ (see Kralj-Iglič et al., 2001b, 2002b). Besides in the final stage of the vesicle burst and consequent membrane solubilization at higher $C_{12}E_8$ concentrations, the general characteristics of the observed $C_{12}E_8$-doped POPC vesicle shape transformation differ from the corresponding transformation of the pure POPC vesicle also in some other important aspects. The fluctuations of the vesicles seem to be stronger when $C_{12}E_8$ molecules are added to the suspension of vesicles (see Fig. 1) than in the absence of $C_{12}E_8$ (see Kralj-Iglič et al., 2001b, 2002b). Also, the vesicle shapes seem to be more irregular (non-axisymmetric) with characteristic sharp edges (Fig. 1).

4. Discussion and conclusions

A complete picture of the dynamics of the POPC vesicle shape transformations and burst given in Figs. 1–6 seems at this point beyond our understanding. However, we can point out some facts that can be deduced with a certain confidence. The shape transformation of the vesicle protrusion is usually slow so that the characteristic time for the mechanical relaxation of the vesicles is always much shorter than the time of the protrusion shortening (Kralj-Iglič et al., 2002b). Therefore, the observed transient vesicle shapes may be considered as quasi-equilibrium (Kralj-Iglič et al., 2002b; Božič et al., 2002) while the observed giant vesicle shape transformation may be described as a sequence of shapes corresponding to the minimum of elastic energy (Kralj-Iglič et al., 2002b):

$$F = F_b + F_d, \tag{1}$$

where F_b is the isotropic bending energy (Canham, 1970; Helfrich, 1974; Evans and Skalak, 1980) and F_d is the deviatoric bending energy (Kralj-Iglič et al., 2002b).

There are related phenomena where beadlike shapes corresponding to transient exited states were produced by a sudden tensions in the long membrane tubes that are induced either by laser tweezers (Bar-Ziv and Moses, 1994) or by mechanical manipulation (Evans and Rawicz, 1990). These beadlike or undulated structures are unstable excited states of the membrane (Bar-Ziv and Moses, 1994) which are relaxed after certain time, depending on the membrane shape. Slight undulations are relaxed in seconds while sphere-like beads connected by thin tubular part are relaxed in minutes (Bar-Ziv and Moses, 1994). In our case the time of relaxation is much longer and also no sudden tension was induced in the membrane which may lead to unstable excited states (Goldstein, 1996). Therefore, in spite of the certain characteristics of transient states our vesicles pertain more to quasi-equilibrium states (Kralj-Iglič et al., 2002b; Božič et al., 2002) than to transient excited states. Also, the observed oscillations of the width of necks (Figs. 1 and 2) can be considered as the oscillations around the equilibrium shape (Iglič and Kralj-Iglič, 2003; Božič et al., 2002; Kralj-Iglič et al., 2001b).

The transformation between the equilibrium shapes of closed lipid bilayer vesicles corresponding to the minimal elastic energy has been extensively studied in the past (Canham, 1970; Deuling and Helfrich, 1976; Evans and Skalak, 1980; Lipowsky, 1991; Miao et al., 1994; Iglič et al., 1999, 2000; Kralj-Iglič et al., 2002b). The isotropic Helfrich-Evans bending energy of the membrane bilayer F_b is the superposition of the local term (Canham, 1970; Helfrich, 1974; Evans, 1974) and the non-local term (Evans and Skalak, 1980; Helfrich, 1974) which results from different dilatation of the monolayers (Evans and Skalak, 1980) and may

be written in the following form (Evans and Skalak, 1980; Helfrich, 1974; Stokke et al., 1986):

$$F_b = \frac{k_c}{2}\int (2H - \bar{C}_0)^2 dA + k_G \times \int C_1 C_2 dA + k_n A(\langle H\rangle)^2, \quad (2)$$

where

$$\langle H\rangle = \frac{1}{A}\int H\, dA, \quad (3)$$

is the average mean curvature (Iglič and Kralj-Iglič, 2003), $H = (C_1 + C_2)/2$ is the mean curvature of the membrane at a chosen point, C_1 and C_2 are two principal curvatures (where the indexes 1 and 2 are chosen so that C_1 is larger than C_2), k_c is the coefficient of local bending rigidity, k_G is the Gaussian coefficient of bending rigidity while k_n is the coefficient of non-local bending rigidity (Evans and Skalak, 1980). The integration is performed over the membrane area A. The non-zero (effective) spontaneous curvature of the bilayer $\bar{C}_0$ (Helfrich, 1974; Mukhopadhyay et al., 2002; Miao et al., 1994; Kralj-Iglič et al., 1996) may be the consequence of the bilayer asymmetry due to different environments on the two sides of the bilayer, due to different compositions and due to different number of molecules in the two constituent monolayers (Helfrich, 1974; Evans and Skalak, 1980). The Helfrich–Evans isotropic bilayer bending energy (Eq. (2)) can be rewritten in the equivalent form:

$$F_b = \frac{k_c}{2}\int (2H)^2 dA + k_G \times \int C_1 C_2 dA + k_n A(\langle H\rangle - H_0)^2, \quad (4)$$

where the spontaneous average mean curvature H_0 is proportional to the parameter $\bar{C}_0$. For thin and not too strongly curved bilayers the average mean curvature $\langle H\rangle$ is proportional to the area difference between the two monolayers: $\langle H\rangle = \Delta A/2A\delta$, where δ is the distance between the two monolayer neutral surfaces. Using the above relation between ΔA (Sheetz and Singer, 1974; Beck, 1978; Evans and Skalak, 1980) and $\langle H\rangle$ the energy F_b can be expressed also as the function of the area difference ΔA and effective relaxed area difference $\overline{\Delta A}_0 = 2A\delta H_0$ (Mukhopadhyay et al., 2002; Miao et al., 1994; Stokke et al., 1986). $\overline{\Delta A}_0$ and H_0 depend on asymmetry in composition, environment and number of molecules between both monolayers. In accordance with the previous considerations (Helfrich, 1974; Miao et al., 1994), it was established that the effects of bilayer asymmetry due to different environments on the two sides of the bilayer, due to different compositions of the monolayers and due to different number of molecules in the two constituent monolayers should not enter in the expression for the isotropic bending energy of the bilayer (Eqs. (2) and (4)) independently but only in the form of the (effective) spontaneous curvature of the bilayer $\bar{C}_0$ or alternatively in the form of spontaneous average mean curvature H_0 (or effective relaxed area difference $\overline{\Delta A}_0$) (Mukhopadhyay et al., 2002).

The deviatoric bending energy F_d can be written in the form (Kralj-Iglič et al., 2002b; Iglič and Kralj-Iglič, 2003):

$$F_d = -2m_0 kT\int \ln\left(I_0\left(\frac{\xi + \xi^*}{2kT} D_m D\right)\right) dA, \quad (5)$$

where ξ and ξ^* are constants describing the interaction of a single lipid molecule with the surrounding molecules, m_0 is the area density of lipid molecules in membrane mononolayer, I_0 is the modified Bessel function, $D = (C_1 - C_2)/2$ is the curvature deviator (Kralj-Iglič et al., 2002a; Evans and Skalak, 1980), $D_m = (C_{1m} - C_{2m})/2$ is the curvature deviator intrinsic to the single lipid molecule, C_{1m} and C_{2m} are the principal curvatures of the intrinsic shape of the single lipid molecule (Kralj-Iglič et al., 2002a,b). In accordance with the definitions of C_1 and C_2, where C_1 is the larger of the two principal curvatures, the curvature deviator D is always positive (Kralj-Iglič et al., 2002a).

It can be seen that the elastic energy of the bilayer membrane is in general the function of the two invariants (of the first order) of the diagonalized curvature tensor (Kralj-Iglič et al., 2002a,b; Fischer, 1991): the mean curvature H and the curvature deviator D. It should be noted that the Gaussian curvature can be expressed by H and D as follows $C_1C_2 = H^2 - D^2$. For the sake of simplicity, we treat the membrane bilayer as incompressible, therefore, the elastic energy of stretching (Evans and Skalak, 1980) was neglected in Eq. (1).

As it can be seen in Fig. 1A–C in early stages of POPC vesicle shape transformation the protrusions of the vesicles are not beadlike but tubular (Kralj-Iglič

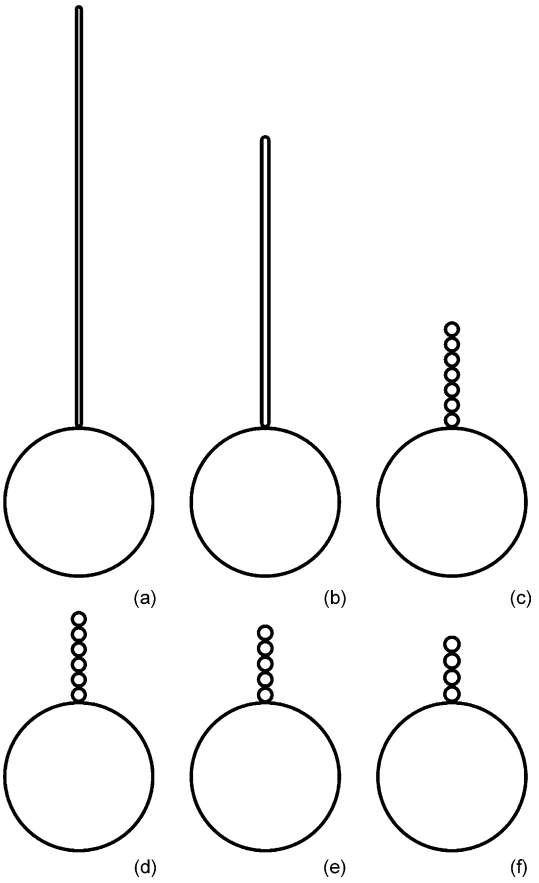

Fig. 7. A sequence of axisymmetric equilibrium vesicle shapes corresponding to minimal membrane elastic energy F at constant vesicle volume and area for different values of normalized average mean curvature $\langle h \rangle$: 1.7 (a), 1.51 (b), 1.47 (c), 1.44 (d), 1.40 (e) and 1.36 (f). The relative cell volume $v = 0.95$, $RD_m = 2000$. The non-local term in F_b was not taken into account in minimization procedure.

et al., 2001b, 2002b). For comparison with these experimental observations, Fig. 7 shows the calculated equilibrium vesicle shapes corresponding to the early stages of POPC vesicle shape transformation where some of the predicted shapes of the vesicle protrusions are not beadlike but tubular (Fig. 7a and b). The calculated shapes in Fig. 7 correspond to the minimal membrane elastic energy $F = F_b + F_d$ (Eq. (1)) at different values of normalized average mean curvature $\langle h \rangle = R\langle H \rangle$, where $R = \sqrt{A/4\pi}$. Normalized average mean curvature $\langle h \rangle$ is equal to the normalized area difference between the membrane monolayers $\Delta a = \Delta A/8\pi\delta R$. The equilibrium vesicle shapes at given $\langle h \rangle$ and at given relative vesicle volume $v = 3V/4\pi R^3$ are calculated as described in detail elsewhere (Kralj-Iglič et al., 2002b). As the non-local contribution to the isotropic bending energy (third term in Eq. (4)) does not influence the calculated equilibrium vesicle shape at given $\langle h \rangle$ (Iglič et al., 1999) in this work for the sake of simplicity the non-local term in the energy F_b was not taken into account in minimization procedure.

It can be seen in Fig. 7 that at higher values of $\langle h \rangle$ the calculated equilibrium vesicle shapes corresponding to the minimum of the membrane elastic energy F (Eq. (1)) have a long tubular protrusion. As the membrane area and the enclosed volume of the vesicles are fixed the length of these tubular protrusions decreases while their diameter increases with decreasing of $\langle h \rangle$ (Fig. 7). Since at high values of $\langle h \rangle$ the tubular protrusions are very thin they have large average curvature deviator $\langle D \rangle = 1/A \int D \, dA$ (Kralj-Iglič et al., 2002b). For such thin tubular protrusion the absolute value of the negative deviatoric bending energy F_d (Eq. (5)) is therefore large enough to compensate for the less favourable high bending energy of the thin cylindrical shape of the protrusion. On the other hand, for lower $\langle h \rangle$, a tubular protrusion of the same membrane area and enclosed volume would be shorter and broader, and therefore, its average curvature deviator $\langle D \rangle$ would be lower. The corresponding deviatoric energy of the thick tubular protrusion would be therefore too small (i.e. negligible) to favour the tubular shapes of the protrusions. Consequently, at lower $\langle h \rangle$ the shape with the beadlike protrusion has lower free energy F (Fig. 7c–f) in accordance with experimental observation (Fig. 1). At a chosen intrinsic anisotropy of the single lipid molecule D_m, the protrusion composed of the chain of small spheres is energetically more favourable below a certain value of $\langle h \rangle$ while above this threshold the tubular shape of protrusions is favoured (Fig. 7) (Kralj-Iglič et al., 2002b). In the case presented in Fig. 7, the shapes of the vesicle protrusion have the beadlike character for the values of $\langle h \rangle$ smaller than 1.51.

Based on the results presented in Fig. 7 it can be concluded that a possible mechanism that can explain the stability of the observed long thin tubular protrusions (Fig. 1) and the shape transformation of the tubular protrusion in the beadlike protrusion (shown

in Fig. 1) may be the deviatoric elasticity (Eq. (5)) which is the consequence of the orientational ordering of the membrane components in the membrane bilayer of the thin tubular protrusions of the vesicles (Kralj-Iglič et al., 2002b; Iglič and Kralj-Iglič, 2003). The observed transformation of the tubular protrusion into the beadlike protrusion cannot be explained only by the minimization of the Helfrich–Evans isotropic bilayer bending energy F_b (Eq. (4)) (Kralj-Iglič et al., 2002b; Božič et al., 2002). This result is in accordance with the results of previous studies which show that there is no evidence that the vesicles with tubular protrusions are low F_b energy structures (Kralj-Iglič et al., 2002b; Miao et al., 1991).

Fig. 8 shows the calculated equilibrium vesicle shapes corresponding to the minimal isotropic bending energy F_b at different values of normalized average mean curvature $\langle h \rangle$. The equilibrium vesicle shapes at given $\langle h \rangle$ and at given relative vesicle volume v are calculated as described in detail elsewhere (Iglič et al., 1999; Kralj-Iglič et al., 2002b). Again, for the sake of simplicity, the non-local term in the energy F_b was not taken into account in minimization procedure. At relative volume $v = 0.85$, the chosen values of $\langle h \rangle$ in Fig. 8 are small enough so that the tubular protrusions are not stable. Therefore, the deviatoric energy F_d (Eq. (5)) was not considered in the minimization procedure although it might be important in stabilization of the finite necks connecting the beads (Kralj-Iglič et al., 2002b).

Shapes a–d and shapes k–n given in Fig. 8 are the limiting shapes composed of large mother sphere and the protrusion (invagination) composed of small spheres connected by infinitesimal necks (Iglič et al., 1999; Kralj-Iglič et al., 2002b). The beadlike protrusions (invagination) of the limiting equilibrium vesicle shapes with minimal isotropic bending energy F_b given in Fig. 8 are composed of small spheres connected by infinitesimal necks (Kralj-Iglič et al., 2002b). It has been shown that also the protrusions of the intermediate equilibrium vesicles shapes with minimal F_b (i.e. the protrusions of the equilibrium shapes between the limiting shapes a–b, b–c and c–d given in Fig. 8) have the beadlike shape with very thin connecting necks (Božič et al., 2002; Miao et al., 1991) which is however not in accordance with experimental evidence. The observed necks are usually broader than the theoretically predicted necks of stable vesicle shapes (Božič et al., 2002). Namely, it can be clearly seen in Figs. 1–3 that the observed beadlike protrusions of the intermediate vesicle shapes have mostly thick necks. The observed thick necks can be the consequence of the membrane thermal fluctuation around the stable limiting vesicle shapes composed of spherical mother cell and spherical daughter vesicles connected by very thin neck (Iglič and Kralj-Iglič, 2003).

The previously observed (Käs and Sackmann, 1991; Kralj-Iglič et al., 2001b; Iglič and Kralj-Iglič, 2003) instability of pear-shaped vesicles close to the limiting shape composed of spherical mother cell and spherical daughter vesicles connected by very thin neck, i.e. the oscillation of the neck width (Figs. 1 and 2), and also the strong stability of this limiting vesicle shapes if they are reached (Fig. 2X) cannot be explained within the standard isotropic bending elasticity models (Käs and Sackmann, 1991; Miao et al., 1991). The observed phenomena can possibly be explained by stabilization of the neck by orientational ordering of the membrane components in the neck (Kralj-Iglič et al., 1999, 2001a, 2002b; Iglič and Kralj-Iglič, 2003), i.e. due to negative contribution of the deviatoric bending energy in the neck F_d (Eq. (5)). If the vesicle shape is close to the limiting shape (Fig. 2X), the fluctuations of such vesicles are significantly reduced due to geometrical constraints, leading to the increased stability of such shape.

The formation of $C_{12}E_8$-phospholipid membrane inclusions (clusters) due to cooperative interaction of $C_{12}E_8$ with neighboring lipid molecules (Heerklotz et al., 1998; Iglič and Kralj-Iglič, 2003) may lead to decrease of the membrane-bending rigidity (Otten et al., 2000). Consequently, the fluctuations of the vesicles may become very strong as it can be seen in Fig. 1. It has been suggested that the softening of the membrane bilayer by $C_{12}E_8$ (Otten et al., 2000) may be the consequence of the $C_{12}E_8$ induced perturbations in the region of phospholipid acyl chains of the membrane bilayer (Heerklotz et al., 1997, 1998; Thurmond et al., 1994), which are reflected in the changes of the order parameter and of the relaxation parameters of membrane lipids (Otten et al., 2000; Fošnarič et al., 2002). In the case of the erythrocyte membrane, the $C_{12}E_8$ induced perturbation of phospholipid acyl chains is reflected also in the changes of the proportions of the membrane lipid domains (Fošnarič

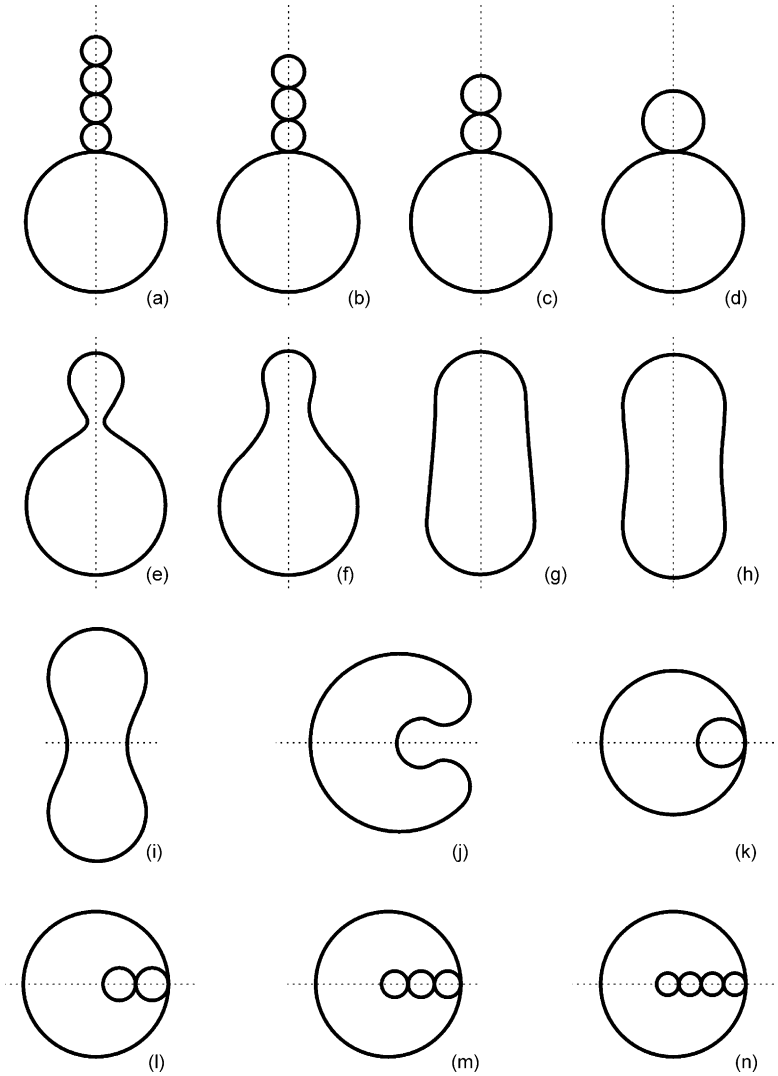

Fig. 8. A sequence of axisymmetric equilibrium vesicle shapes corresponding to minimal isotropic local bending energy at constant vesicle volume and area for different values of normalized average mean curvature $\langle h \rangle$: 1.62 (a), 1.53 (b), 1.43 (c), 1.30 (d), 1.25 (e), 1.17 (f), 1.086 (g), 1.085 (h), 1.02 (i), 0.77 (j), 0.66 (k), 0.53 (l), 0.43 (m) and 0.34 (n). The relative cell volume $v = 0.85$. The broken lines show the axes of rotational symmetry. Note that the axis of rotational symmetry changes its direction for 90 degrees between the shapes *h* and *i*.

et al., 2002). In accordance with this assumption, it was observed that increasing of $C_{12}E_8$ concentration in POPC/$C_{12}E_8$ mixture induces a transition from lamellar to hexagonal phase (Otten et al., 1995).

As described in the Section 2, in the interior of our vesicles is pure sucrose solution while outside of the vesicles is the mixed solution of glucose and sucrose. Therefore, the vesicles containing the solution of the heavier sugar sucrose sank to the bottom of the observation chamber due to gravitational force (Döbereiner et al., 1999) while the long protrusion is usually in the horizontal position (Kralj-Iglič et al., 2002b). This made the observation of the protrusion easier. On the other hand, if the large mother vesicle

touches the bottom of the observation chamber the shape of such vesicle is influenced by adhesion and gravity (Kraus et al., 1995; Seifert, 1997; Döbereiner et al., 1999). In our case, in the beginning (Figs. 7 and 8a–d) and at the end (Fig. 8k–n) of the observed vesicle shape transformation (Figs. 1–4) the mother vesicle is rather rigid and spherical, therefore, the contact area of the mother vesicle with the glass cannot be very large. However, in the middle of the observed shape transformation the mother vesicle is not spherical (Figs. 3A–I and 8f–j) and fluctuate, therefore, the contact area of the mother vesicle with the glass could be larger and also the influence of the adhesion and gravity on these intermediate vesicle shapes might be important (Kraus et al., 1995; Seifert, 1997; Seifert and Lipowsky, 1990; Döbereiner et al., 1999). However, as it has been shown recently that qualitatively the same shape transformation as presented in Fig. 1 was observed in pure water (Kralj-Iglič et al., 2002b) where the vesicles were floating in the observation chamber. Although the details of the shape can be expected to depend on the adhesion of the vesicles and the gravitational field, we believe that these effects are minor in determining the essence of the observed shape transformation presented in Fig. 1.

The shape transition between the prolate dumbbell vesicle shape (Fig. 3D) and the oblate vesicle shape (Fig. 3I) involves non-axisymmetric shapes (Peterson, 1989; Kralj-Iglič et al., 1993). Within the calculated sequence of axisymmetric vesicle shape with minimal isotropic bending energy F_b given in Fig. 8 the intermediate non-axisymmetric vesicle shapes between the prolate dumbbell shapes (shape h in Fig. 8) and the oblate shape (shape i in Fig. 8) have not been predicted (Miao et al., 1994). Following the theoretical results for vesicle shape transformations for nearly spherical vesicles (Peterson, 1989), the existence of non-axisymmetric ellipsoid bilayer vesicle shapes was also proved at smaller vesicle relative volumes (Kralj-Iglič et al., 1993).

By comparing the observed sequence of the vesicle shapes (Figs. 1–4) and the calculated equilibrium shapes given in Figs. 7 and 8, it can be concluded that the average mean curvature of the vesicle $\langle H \rangle$ is continuously decreased during the described vesicle shape transformation. The observed vesicle shape transformations may be therefore driven by continuous decreasing of the spontaneous average mean curvature H_0 (Eq. (4)) which may depend among others on the difference in the physical properties of the inner and outer solution, on the difference in composition of the both membrane monolayers and on the difference in the number of molecules in both membrane monolayers. The decrease of the number of the phospholipid molecules in the outer lipid layer may be induced by the inequality of the chemical potential of the phospholipid molecules in the outer solution and in the outer membrane layer which causes a decrease of H_0, and consequently, the decrease of the average mean curvature of the vesicle $\langle H \rangle$. Other possible mechanisms that were suggested to contribute to this are the drag of the lipid molecules from the outer solution by the glass walls of the chamber, chemical modification of the phospholipid and phospholipid flip-flop (Kralj-Iglič et al., 2001b). If the final vesicle shape is composed of a spherical mother cell and a spherical endovesicles, the average membrane curvature $\langle H \rangle$ cannot be further decreased due to geometrical constraints which may lead to excess membrane tensions and consequent membrane leakage (Holopainen et al., 2002) and solubilization (Fig. 6). The probability for membrane leakage is increased with increasing concentration of $C_{12}E_8$ (Fig. 6).

It can be therefore assumed that the tubular/beadlike character of the vesicle protrusion depends on the loss of lipid molecules from the outer membrane layer. The observed increase of the speed of the vesicle shape transformation in the presence of $C_{12}E_8$ in the suspension may be the consequence of the drag of POPC molecules by $C_{12}E_8$ from the outer membrane lipid monolayer (Nomura et al., 2001) and the subsequent formation of mixed POPC-$C_{12}E_8$ micelles in the outer solution (Nomura et al., 2001; Funari et al., 2001; Alberts et al., 1994; Schreier et al., 2000).

The change in osmolarity in the outer solution due to $C_{12}E_8$ can cause the change in the vesicle volume. Also, the area of the vesicles may be changed due to incorporation of the $C_{12}E_8$ or extraction of the lipids from the membrane by $C_{12}E_8$ (Nomura et al., 2001). The change of the vesicle area (A) and the vesicle volume (V) is reflected in the change of the relative vesicle volume $v = 3V/4\pi R^3$ ($R = \sqrt{A/4\pi}$) and therefore also in the vesicle shape and shape transformations. At chosen normalized average mean curvature $\langle h \rangle$, the thickness of the calculated tubular protrusions of the vesicles (Fig. 7) is larger for the

smaller relative volumes v (not shown on the figures). This means that at the smaller relative volumes v the predicted shape transformation of the tubular protrusion into the beadlike protrusion (Fig. 7b and c) would occur at larger values of $\langle h \rangle$ (i.e. at the earlier times) than at larger relative volumes v. Also, it can be concluded from Figs. 7 and 8 that at the given number of the beads the protrusion is composed of smaller beads while the radius of the mother vesicle is slightly larger at larger relative volumes of the vesicle.

It has been shown recently that the intrinsic molecular shape of the membrane constituents (described by C_{1m} and C_{2m}) may be an important factor for determining the stability of membrane pores (Iglič and Kralj-Iglič, May, 2003). In line with these theoretical predictions, the observed increase of membrane leakage by $C_{12}E_8$ (Kandušer et al., 2003) can be explained by the specific role of $C_{12}E_8$ in stabilization of membrane pores. It was proposed that the anisotropic intrinsic molecular shape of phospholipid-$C_{12}E_8$ clusters (inclusions) may play a central role in stabilization of the membrane pore (Kandušer et al., 2003).

In line with the above experimental observation, we observed in this work that $C_{12}E_8$ may induce holes in membrane bilayer. The similar creation of the holes in the vesicles membrane and the burst of the giant phospholipid vesicles at higher $C_{12}E_8$ concentrations as observed in the present work (Fig. 6) have been detected also before in large spherical phospholipid vesicles (Nomura et al., 2001). The $C_{12}E_8$ induced holes in membrane bilayer have been seen also in small lipid vesicles (Johnsson and Edwards, 2000).

In conclusion, we have recorded for the first time the complete sequence of $C_{12}E_8$-doped POPC vesicle shapes starting from initial spherical shape with a long thin tubular protrusion, through undulated (bead-like) protrusions, prolate dumbbell shapes, oblate shapes to final spherical shape with invagination(s)(Figs. 1–5). The shape of invagination was usually spherical, however, also non-spherical, e.g. undulated, tubular or torocytic shapes of endovesicles were observed. From comparison between the observed sequence of vesicle shapes and the sequence of calculated shapes given in Figs. 7 and 8, it is evident that the average membrane curvature is continuously decreasing during this process. The non-ionic surfactant $C_{12}E_8$ caused the observed vesicle shape transformations to be faster than the corresponding transformation of pure POPC vesicles while the necks of the bead-like protrusions seem to be thicker with added $C_{12}E_8$ in comparison to the situation without $C_{12}E_8$ (see Kralj-Iglič et al., 2001b, 2002b). In accordance with the previous observation indicating the softening of the membrane bilayer due to the intercalated $C_{12}E_8$, we observed that the fluctuations of the vesicles are stronger after addition of $C_{12}E_8$. In some cases, the vesicles have characteristic edges (Fig. 1) which have not been observed in the absence of $C_{12}E_8$. In accordance with the recent observations (Nomura et al., 2001), we have recorded also the membrane leakage and burst of POPC vesicles at higher concentrations of $C_{12}E_8$.

References

Alberts, B., Bray, D., Lewis, J., Raff, M., Roberts, K., Watson, J.D., 1994. Molecular Biology of Cell, Garland Publishing, New York.

Angelova, M.I., Soleau, S., Meleard, P., Faucon, J.F., Bothorel, P., 1992. Preparation of giant vesicles by external AC electric field: kinetics and application. Prog. Colloid Polym. Sci. 89, 127–131.

Beck, J.S., 1978. Relations between membrane monolayers in some red cell shape transformations. J. Theor. Biol. 75, 487–501.

Bar-Ziv, R., Moses, E., 1994. Instability and "pearling" states produced in tubular membranes by competition of curvature and tension. Phys. Rev. Lett. 73, 1392–1395.

Božič, B., Gomišček, G., Kralj-Iglič, V., Svetina, S., Zekš, B., 2002. Shape of phospholipid vesicles with beadlike protrusions. Eur. Biophys. J. 31, 487–496.

Canham, P.B., 1970. The minimum energy of bending as a possible explanation of the biconcave shape of the human red blood cell. J. Theor. Biol. 26, 61–81.

Deuling, H.J., Helfrich, W., 1976. The curvature elasticity of fluid membranes: a catalogue of vesicle shapes. J. Phys. (France) 37, 1345–1355.

Döbereiner, H.G., Selchow, O., Lipowsky, R., 1999. Spontaneous curvature of fluid vesicles induced by trans-bilayer sugar asymmetry. Eur. Biophys. J. 28, 174–178.

Evans, E.A., 1974. Bending resistance and chemically induced moments in membrane bilayers. Biophys. J. 14, 923–931.

Evans, E.A., Skalak, R., 1980. Mechanics and Thermodynamics of Biomembranes. CRC Press, Boca Raton.

Evans, E., Rawicz, W., 1990. Entropy-driven tension and bending elasticity in condensed-fluid membranes. Phys. Rev. Lett. 64, 2094–2097.

Fischer, T., 1991. Bending stiffness of lipid bilayers. III. Gaussian curvature. J. Phys. II (France) 2, 337–343.

Fošnarič, M., Nemec, M., Kralj-Iglič, V., Hägerstrand, H., Schara, M., Iglič, A., 2002. Possible role of anisotropic membrane inclusions in stability of torocyte red blood cell daughter vesciles. Coll. Surf. A 26, 243–253.

Funari, S., Nuscher, B., Rapp, G., Beyer, K., 2001. Detergent-phospholipid mixed micelles with a crystalline phospholpid core. Proc. Natl. Acad. Sci. U.S.A. 98, 8938–8943.

Goldstein, R.E., Nelson, P., Powers, T., Seifert, U., 1996. Front propagation in the pearling instability of tubular vesicles. J. Phys. II (France) 6, 767–796.

Helfrich, W., 1974. Blocked lipid exchange in bilayers and its possible influence on the shape of vesicles. Z. Naturforsch. 29c, 510–515.

Heerklotz, H., Binder, G., Lantzsch, G., Klose, G., 1997. Lipid/detergent interaction thermodynamics as a function of molecular shape. J. Phys. Chem. B 101, 639–645.

Heerklotz, H., Binder, H., Schmiedel, H., 1998. Excess enthalpies of mixing in phospholipid-additive membranes. J. Phys. Chem. B 102, 5363–5368.

Holopainen, J.M., Angelova, M.I.T., Kinnunen, P.K.J., 2000. Vectorial budding of vesicles by asymmetrical enzymatic formation of ceramide in giant liposomes. Biophys. J. 78, 830–838.

Holopainen, J.M., Angelova, M.I., Söderlund, T., Kinnunen, P.K.J., 2002. Macroscopic consequences of the action of phospholipase C on giant unilamellar liposomes. Biophys. J. 83, 932–943.

Iglič, A., Kralj-Iglič, V., Majhenc, J., 1999. Cylindrical shapes of closed lipid bilayer structures correspond to an extreme area difference between the two monolayers of the bilayer. J. Biomech. 32, 1343–1347.

Iglič, A., Kralj-Iglič, V., Božič, B., Bobrowska-Hägerstrand, M., Hägerstrand, H., 2000. Torocyte shape of red blood cell daughter vesicles. Bioelectrochemistry 52, 203–211.

Iglič, A., Kralj-Iglič, V., 2003. Effect of anisotropic properties of membrane constituents on stable shapes of membrane bilayer structure. In: Ti Tien, H., Ottova, A. (Eds.), Planar Lipid Bilayers (BLMs) and Their Applications. Elsevier, Amsterdam, pp. 143–172.

Johnsson, M., Edwards, K., 2000. Interactions between non-ionic surfactants and sterically stabilised phosphatidyl choline liposomes. Langmuir 16, 8632–8642.

Käs, J., Sackmann, E., 1991. Shape transitions and shape stability of giant phospholipid vesicles in pure water induced by area-to-volume changes. Biophys. J. 60, 825–844.

Kandušer, M., Fošnarič, M., Šentjurc, M., Kralj-Iglič, V., Hägerstrand, H., Iglič, A., Miklavčič, D., 2003. Effect of surfactant polyoxyethylene glycol $C_{12}E_8$ on electroporation of cell line DC3F. Coll. Surf. A 214, 205–217.

Kralj-Iglič, V., Svetina, S., Zekš, B., 1993. The existence of non-axisymmetric bilayer vesicle shapes predicted by the bilayer couple model. Eur. Biophys. J. 22, 97–103.

Kralj-Iglič, V., Svetina, S., Žekš, B., 1996. Shapes of bilayer vesicles with membrane embedded molecules. Eur. Biophys. J. 24, 311–321.

Kralj-Iglič, V., Heinrich, V., Svetina, S., Žekš, B., 1999. Free energy of closed membrane with anisotropic inclusions. Eur. Phys. J. B 10, 5–8.

Kralj-Iglič, V., Iglič, A., Bobrowska-Hägerstrand, M., Hägerstrand, H., 2001a. Tethers connecting daughter vesicles and parent red blood cell may be formed due to ordering of anisotropic membrane constituents. Coll. Surf. A 179, 57–64.

Kralj-Iglič, V., Gomišček, G., Majhenc, J., Arrigler, V., Svetina, S., 2001b. Myelin-like protrusions of giant phospholipid vesicles prepared by electroformation. Coll. Surf. A 181, 315–318.

Kralj-Iglič, V., Remškar, M., Vidmar, G., Fošnarič, M., Iglič, A., 2002a. Deviatoric elasticity as a possible physical mechanism explaining collapse of inorganic micro and nanotubes. Phys. Lett. A 296, 151–155.

Kralj-Iglič, V., Iglič, A., Gomišček, G., Sevšek, F., Arrigler, V., Hägerstrand, H., 2002b. Microtubes and nanotubes of phospholipid bilayer membrane. J. Phys. A Math. Gen. 35, 1533–1549.

Kraus, M., Seifert, U., Lipowsky, R., 1995. Gravity-induced shape transformation of vesicles. Europhys. Lett. 32, 431–436.

Lieber, M.R., Steck, T.L., 1982. A description of holes in human erythrocyte membrane ghost. J. Biol. Chem. 257, 11651–11659.

Lipowsky, R., 1991. The conformation of membranes. Nature 349, 475–481.

May, S., 2003. A molecular model for the line tension of lipid membranes. Eur. Phys. J. E3, 37–44.

Miao, L., Fourcade, B., Rao, M., Wortis, M., Zia, R.K.P., 1991. Equilibrium budding and vesiculation in the curvature model of fluid lipid vesicles. Phys. Rev. E 43, 6843–6856.

Miao, L., Seifert, U., Wortis, M., Döbereiner, H.G., 1994. Budding transitions of fluid-bilayer vesicles: effect of area difference elasticity. Phys. Rev. E 49, 5389–5407.

Mukhopadhyay, R., Lim, G., Wortis, M., 2002. Echinocyte shapes: bending stretching and shear determine spicule shape and spacing. Biophys. J. 82, 1756–1772.

Nomura, F., Nagata, M., Inaba, T., Hiramatsu, H., Hotani, H., Takiguchi, K., 2001. Capabilities of liposomes for topological transformation. Proc. Natl. Acad. Sci. U.S.A. 98, 2340–2345.

Otten, D., Löbbecke, L., Beyer, K., 1995. Stages of the bilayer-micelle transition in the system phosphatidylcholine-$C_{12}E_8$ as studied be deuterium- and phosphorus-NMR, light scattering and calorimetry. Biophys. J. 68, 584–597.

Otten, D., Brown, M.F., Beyer, K., 2000. Softening of membrane bilayers by detergents elucidated by deuterium NMR spectroscopy. J. Phys. Chem. 104, 12119–12129.

Peterson, M.A., 1989. Deformation energy of vesicles at fixed volume and surface in spherical limit. Phys.Rev. A 39, 2643–2645.

Prete, P.S.C., Malherios, S.V.P., de Paula, E., 2002. Solubilization of human erythrocyte membranes by non-ionic surfactant of the polyoxyethylene alkyl ethers series. Biophys. Chem. 97, 45–54.

Schreier, S., Malherios, S.V.P., de Paula, E., 2000. Surface active drugs: self-association and interaction with membranes and surfactant. Physicochemical and biological aspects. Biochim. Biophys. Acta 1508, 210–234.

Seifert, U., Lipowsky, R., 1990. Adhesion of vesicles. Phys. Rev. A 42, 4768–4771.

Seifert, U., 1997. Configurations of fluid membranes and vesicles. Adv. Phys. 46, 13–137.

Sheetz, M.P., Singer, S.J., 1974. Biological membranes as bilayer couples. A molecular mechanism of drug-erythrocyte interactions. Proc. Natl. Acad. Sci. U.S.A. 72, 4457–4461.

Stokke, B.T., Mikkelsen, A., Elgsaeter, A., 1986. The human erythrocyte membrane skeleton may be an ionic gel. Eur. Biophys. J. 13, 203–218.

Tanaka, T., Tamba, Y., Masum, S.M., Yamashita, Y., Yamazaki, M., 2002. La^{3+} and Gd^{3+} induce shape change of giant unilamellar vesicles of phosphatidylcholine. Biochim. Biophys. Acta 1564, 173–182.

Thurmond, R.L., Otten, D., Brown, M.F., Beyer, K., 1994. Structure and packing of phosphotidylcholine in lamellar and hexagonal liquid-crystalline mixtures with a non-ionic detergent: a wide-line deuterium and phosphorus-31 NMR study. J. Phys. Chem. 98, 972–983.